OPTIMIZATIONS OF AIRFOIL AND WING USING GENETIC ALGORITHM

F. Zhang, S. Chen and M. Khalid
Institute for Aerospace Research (IAR)
National Research Council (NRC)
Ottawa, K1A 0R6, Ontario, Canada
Steve.Zhang@nrc.ca

Keywords: genetic algorithm, aerodynamic optimization, CFD, airfoil, wing

Abstract

The present study demonstrates how the Genetic Algorithm (GA), coupled with the CFD solvers ARC2D for 2D and KTRAN for 3D problems, can successfully be applied to the airfoil and wing aerodynamic drag minimization. The geometry of airfoil and wing sections is represented by a B-spline curve. The actual values of the coordinates of the control nodes for the B-spline curve are designated as the design variables. The NACA0012 airfoil is optimized for a free stream Mach number M_∞=0.30, at which the drag coefficient is reduced by 46.1% for a constant lift coefficient of C_L = 0.55. For the corresponding straight wing, the Mach number is set at M_∞=0.80. The drag coefficient is reduced by 13.5% under the constant lift coefficient of C_L = 0.30. The results demonstrates the powerful reliability and robustness of this technique.

1 Introduction

Computational fluid dynamics (CFD) has matured to a point where it can now be widely used as a key tool for aerodynamic design. Traditionally, most designers adopt a “trial and error” approach when conceptualizing a design and analyzing its performance based on available experiment or empirical data. Numerical optimization methods aim to shorten and simplify this iterative process, while significantly improving the design output.

Optimization techniques can be classified in three different categories: local, global and other methods. Local methods are gradient-based algorithms, which only search one part of the design space. Global methods are stochastic methods which take into consideration the entire design space. Genetic algorithm (GA), simulated annealing, random search methods are all considered as global methods. They also have the advantage of operating on discontinuous design space. Other methods are one-shot or inverse methods [1].

Genetic algorithm is a search algorithm based on the principles of natural selection and natural genetics. It utilizes three operators: reproduction, crossover and mutation. Reproduction is a process in which individual chromosomes in a population are copied according to their objective function values. Crossover refers to the exchange of genes between the parent chromosomes. Mutation is a gene change in a chromosome to prevent GA falling into the local optima. The basis of genetic algorithm can be found in reference [2]. It has been applied extensively for aerodynamic design problems [3,4,5,6]

At IAR, optimization techniques have been used to obtain the optimized airfoil shapes [4,5,6]. These studies involved both inverse and drag minimization problems. However, the CFD solver used in these studies was based on Euler equations. In the current work a CFD code for 2D problems, ARC2D [7], which is formatted to handle both Euler and Navier-

Stokes equations, is coupled with the genetic algorithm. Based on these studies, the Genetic Algorithm for aerodynamic optimization is extended towards 3D configurations. A potential flow based CFD solver KTRAN [8], which is suitable for transonic flows and formatted to handle both isolated wing and wing-fuselage configurations, is used to obtain the aerodynamic loads.

2 Genetic Algorithm Operations

In this paragraph, an airfoil is taken as an example to show the Genetic Algorithm operations.

GA works on a coding of the design variables subject to certain performance constraints. In this study, a B-spline curve of the 6^{th} order is used to represent the airfoil geometry. The actual values of the x and y coordinates of the control nodes for the B-spline curve are designated as the design variables (Figure 1). There are 8 control points for each of the lower and upper sides of the airfoil. Generally, we consider a given initial shape, which is precisely defined by the coordinates of the shape points rather than the control points. The first step is then to find the control points based on the initial shape coordinates by using the least square function method.

A certain number of airfoils (wings) consist of a population. An airfoil (wing) is a chromosome in the population. As suggested in reference [9], the small population size by using Micro-Genetic Algorithm (μGA) can facilitate fitness convergence, while frequent regeneration of new population members enhances the algorithm's capability to void local optima. In this study, this technique was also used. The population size is set to 10. The starting population is generated by mutation from the original airfoil (wing) which is to be optimized.

Fitness evaluation is the basis for GA search and selection procedure. GA aims to reward individuals (chromosomes) with high fitness values and to select them as parents to reproduce offspring. The purpose of optimization in this study is to reduce the drag of an airfoil or a wing for a given lift. Therefore, the ratio of the lift and drag coefficients is used as the fitness value (objective function). Parents are chosen based on the Roulette wheel method where the probability of a parent being chosen is proportional to its fitness value. Each pair of parents produces one offspring (chromosome) by crossover. Then mutation is applied to the offspring. After a new population is produced, the fitness of each member is compared to that of the parent generation and the best members (elitism) are assigned to be the new generation.

A simple one-point crossover scheme is applied. The crossover point is selected randomly. Figure 2 shows how the crossover operates. Some design variables (control nodes) of the kid-airfoil are from dad-airfoil (squares) and some from mom-airfoil (crosses). The probability of the crossover is set at 80%, as the use of smaller values was observed to deteriorate the GA performance [5].

Mutation is carried out by randomly selecting a gene (control node) and changing its value by an arbitrary amount within a prescribed range (1% chord) as illustrated in Figure 3. As this change is applied to the selected node, its neighboring nodes are also adjusted so that the change in slope and curvature of the airfoil profile will not be too abrupt. As discussed by Mantel et. al [10], a high mutation rate of 80% is chosen for better GA performance with real number coding.

To obtain a realistic airfoil geometry constraints, such as the minimum allowable maximum thickness (>8% chord) and the maximum allowed trailing edge angle ($>5^o$, $<20^o$), are imposed. The penalty of the imposed geometry constraints is a loss of a certain amount of drag reduction.

Figure 4 shows the flowchart describing the GA application to aerodynamic optimization for an airfoil (or a wing). The CFD solver (ARC2D or KTRAN) calculates the objective function (C_l/C_d) and sends it to GA, which uses it as a fitness value.

For the 3D wing configuration, a straight wing with constant chord and thickness and an aspect ratio of 1.5 is chosen (Figure 5). The GA operations are applied to each section, defined in the figure, in the same way as that for an airfoil. The procedure only modifies the section shapes.

Numerical experiments showed that the CPU time spent for the GA operations is negligible when compared to the CPU time of flow solution.

3 Grid Generations and CFD Solvers

For the 2D problem, a hyperbolic, 2D grid generator HYGRID was used to generate the grids. A typical C-H grid on a NACA0012 airfoil is shown in Figure 6. The flow field computation was performed out using ARC2D. The code makes use of the implicit pentadiagonal form of the approximate factorization scheme due to Beam and Warming [11]. The multi-step Runge-Kutta scheme due to Jameson, et al. [12] based on the cell-vertex control volume, is also available. Second and fourth order artificial dissipations were used. The corresponding dissipation coefficients were set at 0.25 and 0.64 for a fast convergence. The Baldwin-Lomax turbulence model is available in this code to consider the viscous effects.

For 3D problem, the CFD solver with self-grid generation function, KTRAN, was used, which is based on the modified form of the classical transonic small perturbation equation given by Boppe [13]. It can handle both isolated wing and wing-fuselage configurations. The overall crude grid spans the whole computational domain. The fine grids are imbedded in the global crude grid to model the aircraft components such as wing and fuselage. The purpose of the fine grids is to provide detailed computation in regions where the flow field gradients are large and other flow details are of importance for numerical resolution, while the global crude grid provides a link between the fine grid solutions and the crude grid solutions.

4 Results and Discussions

4.1 2D Airfoil

The drag minimization study was carried out for the airfoil NACA0012 by using GA coupled with grid generator HYGRID and CFD solver ARC2D discussed above. The more challenging Navier-Stokes computation was carried out to demonstrate the reliability and robustness of GA and its successful coupling with the CFD software. The free stream Mach number was set at M_∞=0.30. C_L is set to be 0.55. The angle of attack is allowed to vary during the course of the optimization process [5].

The convergence history of the computation is shown in Figure 7. It was noted after about 650 CFD calls, that the fitness value reaches its converged value. It should be mentioned here that the maximum fitness corresponds to the best member in each generation and the averaged fitness of the entire members in the generation. The trend of the fitness in this figure strongly shows that the optimum was approaching from one generation to another, demonstrating the reliability of the Genetic Algorithm. Figure 8 displays the original NACA0012 airfoil in comparison with the optimized airfoil. Figure 9 shows the corresponding pressure distributions on the airfoil surfaces. The drag coefficient decreased from 0.01484 for the original airfoil to 0.0080 for the optimized airfoil under the fixed lift coefficient C_L = 0.90, which is about 46.1% reduction. The required free stream angle of attack for the original airfoil was computed to

have a value of α = 5.49 degrees to create the required lift coefficient, while it was 1.91 degrees to keep the same lift coefficient for the optimized airfoil. Compared with the original airfoil, the radius of leading edge of the optimized airfoil is greatly reduced. Both smaller angle of attack and leading edge radius result in the decrease of the pressure peak value on the suction surface. At the rearward part of the airfoil, the curvature on the both lower and upper surfaces is increased, which creates the bigger pressure difference between the two surfaces. This would then compensate the lift lost at the forward part of the airfoil in order to keep the lift coefficient constant. The Mach number contours for both original and the resulting optimized airfoils are displayed in Figures 10 and 11, respectively. The maximum local Mach number is reduced from 0.561 for the original airfoil to 0.432 for the optimized airfoil.

4.2 3D Straight Wing

The Genetic Algorithm optimizer was extended to 3D problems based on the 2D problem studies. The computation was performed using CFD solver KTRAN. An interface was established to couple the GA optimizer and the CFD solver and transfer the data between them.

For the safety consideration, the drag minimization was carried out for the NACA0012-based straight wing to validate the optimizer. The wing was represented by 6 sections (Figure 5) in the spanwise direction where GA operations are applied. The optimizations for the more challenging tapered and swept back wings can be carried out in the future from the confidence of successfully investigating this kind of straight wing. For the present study, the free stream Mach number was set at M_∞=0.80. C_L is set to be 0.30. Once again, the angle of attack is allowed to be altered during the optimization process.

The convergence history of the computation is shown in Figure 12, which shows that at least 500 CFD calls are needed to reach to the convergence. Figure 13 displays the original and optimized section shapes of the wing at 4 spanwise locations: η = 0.0, 0.40, 0.60 and 1.0. It is noted that the section shape near the wing root has been changed most, reflecting the different flows in this region from other regions. The most interesting thing is that the shape at the wing root section is quite different from the traditional airfoil shape. This could be changed by optimizing wing-fuselage configuration. Figure 14 gives the corresponding pressure distributions on each section. The computed results produce a shock wave near the leading edge on the upper surfaces of both original and optimized wings. However, the strength of the shock waves for the optimized wing was reduced, from their original values. The location too moved closer to the leading edge. This observation is also substantiated by the Mach number distributions for both original and the resulting optimized wings in Figure 15. As is well known, one of the main contributions to aerodynamic drag in transonic flow is from shock waves. Therefore, in the present study, the reduction of the shock wave in both strength and size contribute to the drag coefficient decrease from 0.03686 for the original wing to 0.03190 for the optimized wing, which represents 13.5% reduction under the fixed lift coefficient C_L = 0.30. It is not surprising that the drag reduction is smaller for a wing than that for an airfoil. For a wing, each wing section must satisfy the geometry constraints, which is equal to imposing much more constraints than those for an airfoil. The more constraints imposed, the less benefits obtained. Close to the trailing edge, the increased curvature on both lower and upper surfaces of the optimized wing creates a greater loading. This would then compensate for the lift lost at the forward part of the wing sections due to the reduced expansion on the upper surface in order to keep the lift coefficient constant. It should be noted that the pressure distribution on each wing section is subject to both streamwise and spanwise (3D effects) flow field influences. These dimensional

aspects of the problem are comprehensively accounted for in the computations.

It was noted that, for the original wing, the free stream angle of attack was set at α = 4.31 degrees to provide a lift coefficient of C_L = 0.30. For the optimized wing, the angle of attack was reduced to α = 3.40 degrees to provide the same lift.

5 Conclusions

The Genetic Algorithm has been successfully applied to the airfoil and wing aerodynamic drag minimization. The results demonstrated the powerful reliability and robustness of the genetic algorithms.

Numerical experiment showed that the CPU time spent for GA operations is negligible when compared to the CPU time of flow solution during the optimization.

The genetic algorithm is independent of the CFD solvers used. This means that the ability of the optimization, to deal accurately and efficiently with subsonic, transonic or supersonic flows, or potential, Euler or Navier-Stokes solutions, strongly depends on the CFD solver.

The optimized airfoil has smaller leading edge radius and angle of attack compared with the original one, leading to the smaller suction peak value on the upper surface.

The optimized 3D wing has weaker shock waves on the upper surface, leading to the smaller drag coefficient.

Both the optimized airfoil and wing have a greater aft loading to compensate for the lift lost at the forward part in order to keep the lift coefficient constant.

6 Acknowledgement

The authors are grateful for the financial support and encouragement from the Department of National Defense.

References

[1] Blaize M, Knight D and Rasheed K. Automated Optimal-Design of 2-Dimensional Supersonic Missile Inlets. Journal of Propulsion and Power, Vol. 14, Iss. 6, 1998.

[2] David E. Goldberg. *Genetic Algorithms in Search, Optimization, and Machine Learning.* Massachusetts, Addison-Wesley, 1989.

[3] Periaux J, Sefrioui M, Stoufflet B, Mantel B and Laporte E. Robust Genetic Algorithms for Optimization Problems in Aerodynamic Design. Genetic Algorithms in Engineering and Computer Sciences, New York, Wiley, 1995.

[4] Tse D and Chan Y. Optimization of Airfoil Design Using a Geometric Genetic Algorithms and a Neural Network. 46th CASI Annual Conference, Montreal, Canada, May, 1999.

[5] Tse D and Chan Y. Multi-Point Design of Airfoils by a Genetic Algorithm. 8th Annual Conference of the CFD Society of Canada, Montreal, Canada, June, 2000.

[6] Tse D and Chan Y. Transonic Airfoil Design Optimization Using Soft Computing Methods. 47th CASI Annual Conference, Ottawa, Canada, April, 2000.

[7] Pulliam T. Euler and Thin Layer Navier-Stokes Codes: ARC2D, ARC3D. Notes for Computational Fluid Dynamics User's Workshop, UTSI E02-4005-023-84, 1984.

[8] Kafyeke F. An Analysis Method for Transonic Flow about Three Dimensional Configurations. Technical Report, Canadair Ltd., Montreal, Canada, 1986.

[9] Krishnakumar K. Micro-Genetic Algorithms for Stationary and Non-Stationary Function Optimization. SPIE Vol. 1196, Intelligent Control and Adaptive Systems, 1989, pp. 289-296.

[10] Mantel B, Periaux J, Sefrioui M, Stoufflet B, Desideri J, Lanteri S, and Marco N. Evolutionary Computational Methods for Complex Design in Aerodynamics. AIAA-98-0222, 36th AIAA Aerospace Sciences Meeting & Exhibit, Jan. 12-15, 1998, Reno, NV.

[11] Beam R and Warming R. An Implicit Finite Difference Algorithm for Hyperbolic Systems in Conservation Law Form. Journal of Computational Physics, Vol. 22, No. 1, September 1976.

[12] Jameson A, Schmidt W and Turkel E. Numerical Solution of the Euler Equations by Finite Volume Methods Using Runge-Kutta Time-Stepping Schemes. AIAA Paper 81-1259, AIAA 14th Fluid and Plasma Dynamics Conference, Palo Alto, California, USA, 1981.

[13] Boppe C. Transonic Flow Field Analysis of Wing Fuselage Configurations. NASA CR 3243, May 1980.

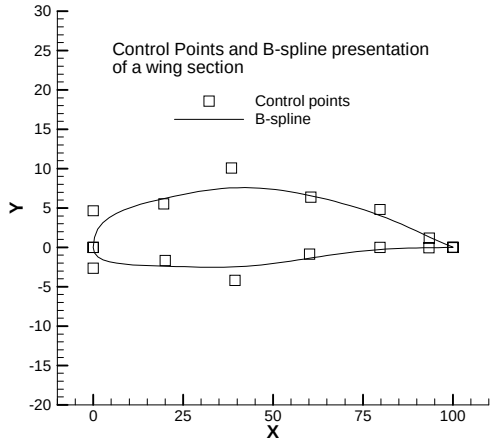

Figure 1. Control points and B-spline presentation of a wing section

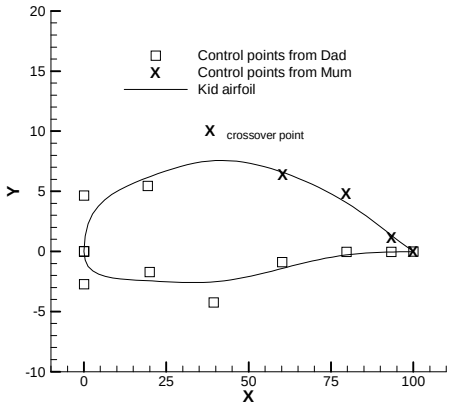

Figure 2. Crossover

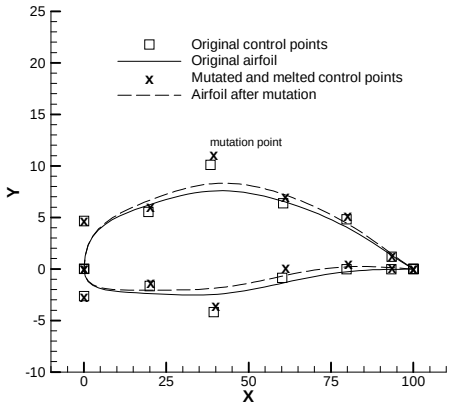

Figure 3. Mutation

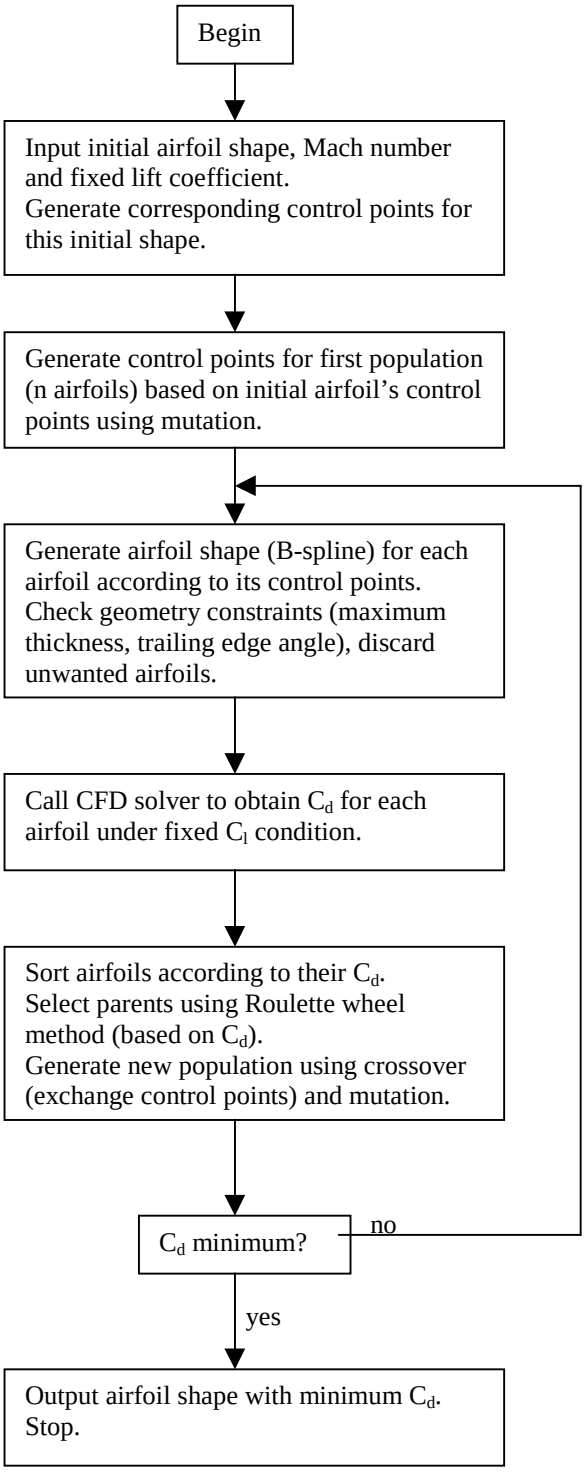

Figure 4. GA Flowchart

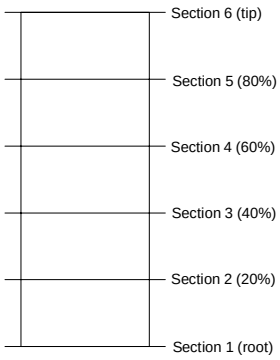

Figure 5. Wing planform

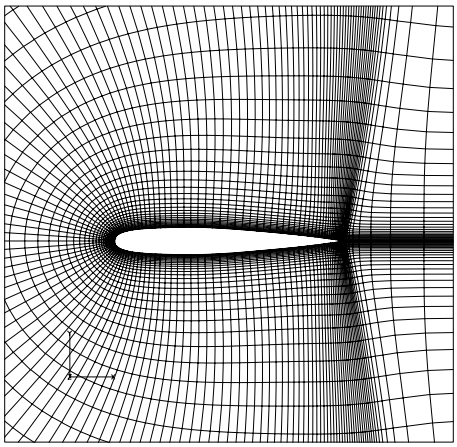

Figure 6. C-H grid around airfoil

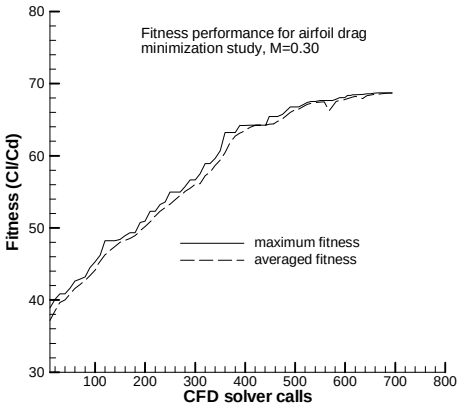

Figure 7. Fitness convergence history for airfoil

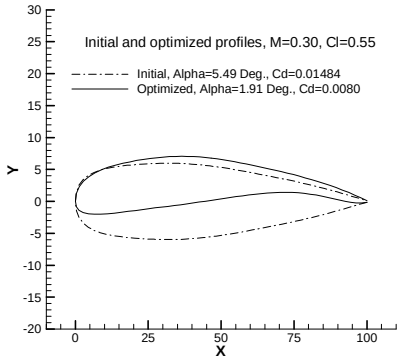

Figure 8. Original NACA0012 and its optimized airfoils, N.S. solution

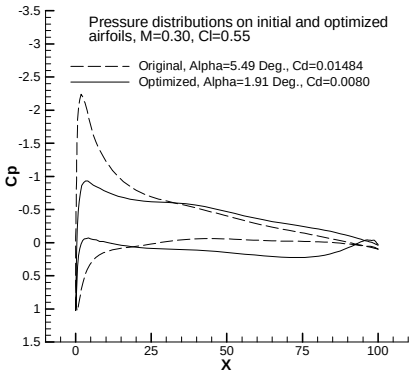

Figure 9. Pressure distributions on the original NACA0012 and its optimized airfoils, N.S. solution

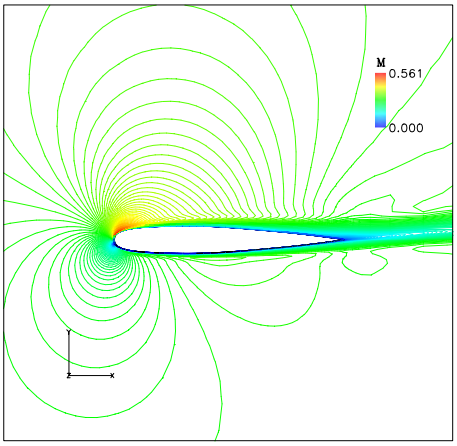

Figure 10. Mach number contours around the original NACA0012 airfoil, N.S. solution

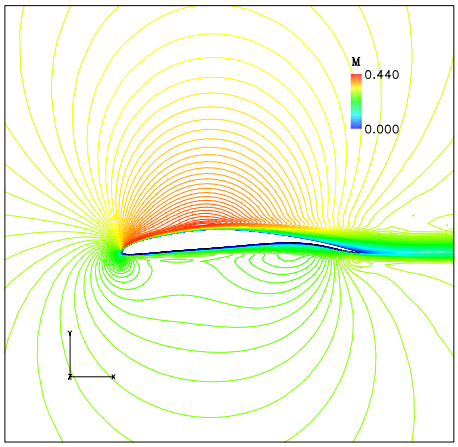

Figure 11. Mach number contours around the optimized airfoil, N.S. solution

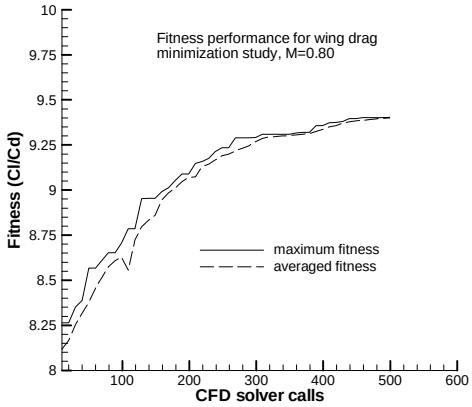

Figure 12. Fitness convergence history for wing

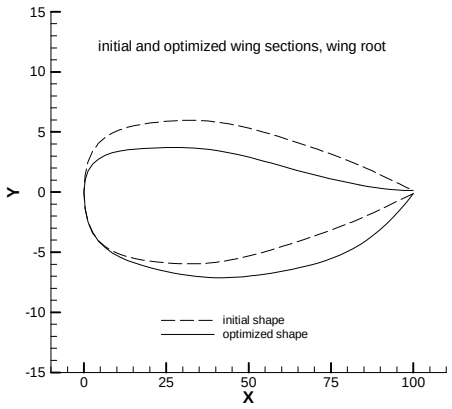

Figure 13(a) Wing root section

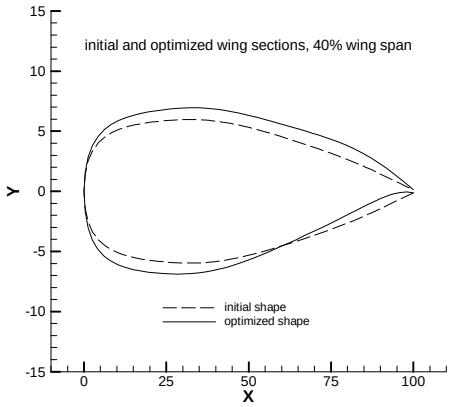

Figure 13(b) 40% wing span section

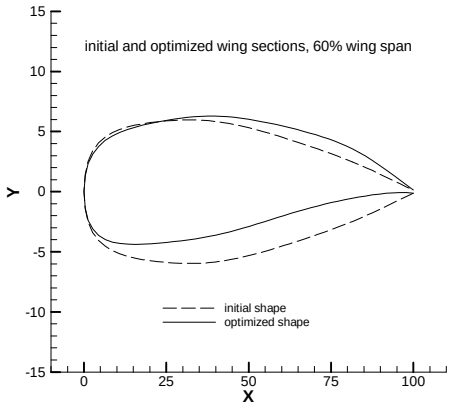

Figure 13(c) 60% wing span section

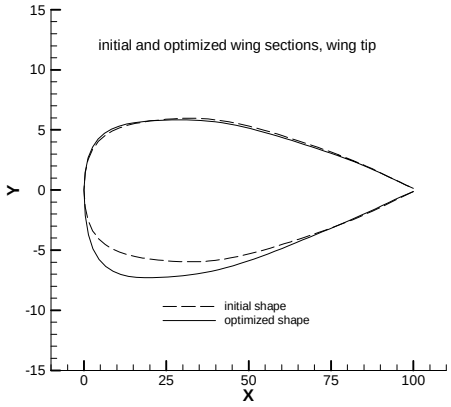

Figure 13(d) Wing tip section

Figure 13. Original wing sections and their optimized sections

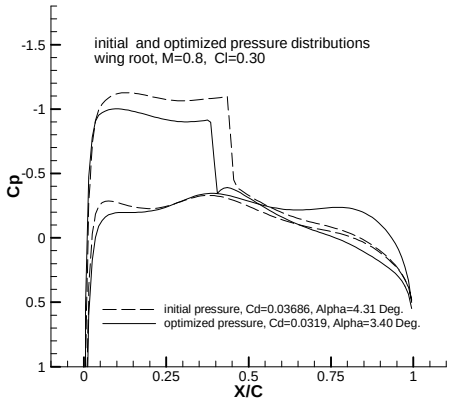

Figure 14(a) Wing root section

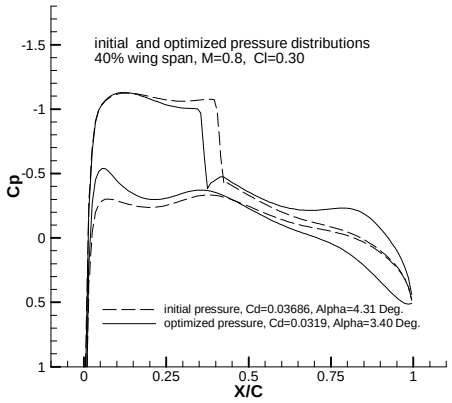

Figure 14(b) 40% wing span section

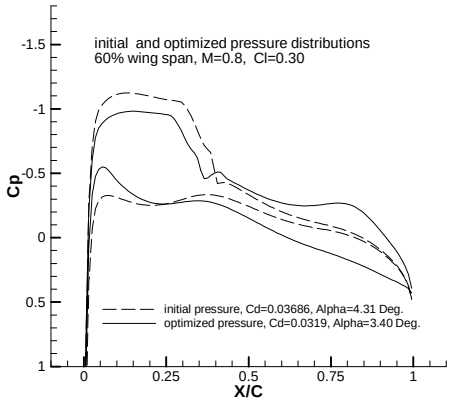

Figure 14(c) 60% wing span section

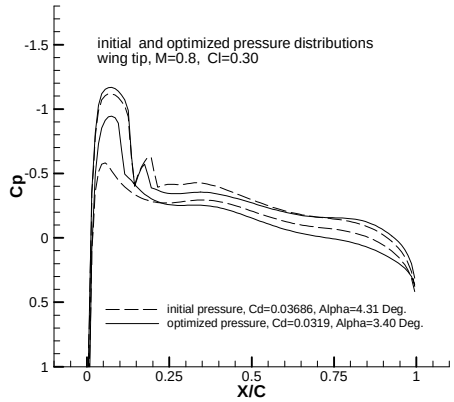

Figure 14(d) Wing tip section

Figure 14. Pressure distributions on the original and optimized wing sections

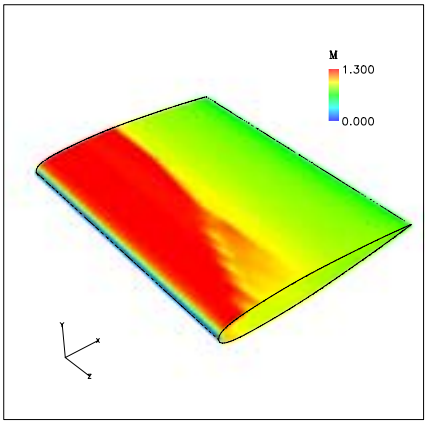

Figure 15. Mach number distributions on the original wing surfaces

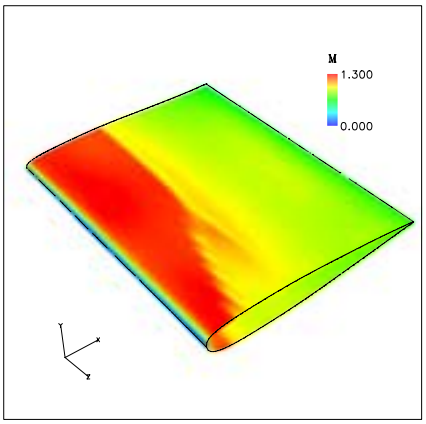

Figure 16. Mach number distributions on the optimized wing surfaces